

Fluctuations and the Clustering of Color Sources

Elena G. Ferreiro

*Departamento de Física de Partículas
Universidade de Santiago de Compostela, Spain*

Contents:

1. Transverse momentum fluctuations
2. Multiplicity fluctuations

in collaboration with Leticia Cunqueiro and Carlos Pajares

WHY EVENT-BY-EVENT FLUCTUATIONS?

Non-statistical event-by-event fluctuations in relativistic heavy ion collisions has been proposed as as **probe of phase instabilities near de QCD phase transition**.

The fluctuations of the mean transverse momentum or mean multiplicity are related to the fundamental properties of the system, so may reveal information about the **QCD phase boundary**.

A phase transition in the evolution of the system created in relativistic heavy ion collisions may lead to a **divergence of the specific heat** which could be observed as **event-by-event fluctuations**.

EVENT-BY-EVENT P_T FLUCTUATIONS

Event-by-event fluctuations of p_T have been measured at SPS and RHIC

Behaviour of the non-statistical fluctuations as a function of the centrality of the collision:

- grow as the centrality increases
- maximum at mid centralities
- decrease at larger centralities

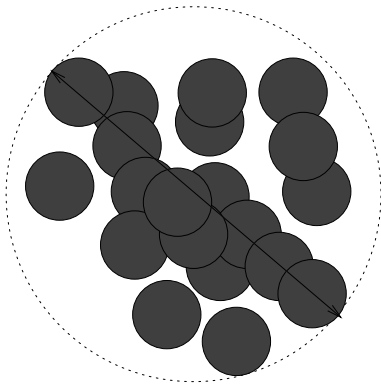
Different mechanisms have been proposed in order to explain those data:

- complete or partial equilibration
- critical phenomena
- production of jets
- string clustering or string percolation.

CLUSTERING OF COLOR SOURCES

(Armesto, Braun, Ferreiro, Pajares, PRL77 (96) 3736)

- In a collision **color strings** are stretched between the colliding partons
- **Strings = color sources** of particles which are successively broken by creation of $q\bar{q}$ pairs from the sea
- **Color strings = small areas** in the transverse space filled with color field created by the colliding partons
- If the density of strings increases \Rightarrow Overlapping in the transverse space
Phenomenon of string fusion and percolation



$$\begin{aligned}\eta &= N_{st} \frac{S_1}{S_A} \\ S_1 &= \pi r_0^2 \\ r_0 &= 0.2 \div 0.3 \text{ fm} \\ \eta_c &= 1.1 \div 1.5.\end{aligned}$$

- **Percolation:** at a critical value η_c of the density the cluster size diverges:
the size of the cluster reaches the size of the system
- Variations of the initial state can lead to a
transition from disconnected to connected color clusters
- **Percolation point = onset of color deconfinement**
- **It says nothing about any subsequent thermalization**
- **The cluster has a higher color charge**, corresponding to the sum of the color charges of the original strings

For a cluster of n overlapping strings:

$$Q_n = \sqrt{\frac{nS_n}{S_1}} Q_1 \quad \mu_n = \sqrt{\frac{nS_n}{S_1}} \mu_1 \quad \langle p_T^2 \rangle_n = \sqrt{\frac{nS_1}{S_n}} \langle p_T^2 \rangle_1$$

IN THE CLUSTERING APPROACH:

The behaviour of the p_T fluctuations can be understood as follows:

- **At low density:** most of the particles are produced by individual strings with the same $\langle p_T \rangle_1$

⇒ **fluctuations are small**

- **At large density** above the critical point: only one cluster

⇒ **fluctuations are not expected either** *"equilibration"*

- **Just below the percolation critical density:** Large number of clusters formed by different number of strings, different size and different $\langle p_T \rangle_n$

⇒ **fluctuations are maximal**

Variables to measure event-by-event p_T fluctuations

F_{p_T} quantifies the deviation of the observed fluctuations from statistically independent particle emission

$$F_{p_T} = \frac{\omega_{data} - \omega_{random}}{\omega_{random}}, \quad \omega = \frac{\sqrt{\langle p_T^2 \rangle - \langle p_T \rangle^2}}{\langle p_T \rangle}$$

$$\phi = \sqrt{\frac{\langle Z^2 \rangle}{\langle \mu \rangle}} - \sqrt{\langle z^2 \rangle}$$

$z_i = p_{T_i} - \langle p_T \rangle$ is defined for each particle

$Z_i = \sum_{j=1}^{N_i} z_j$ is defined for each event

$$F_{p_T} = \frac{\phi}{\sqrt{\langle z^2 \rangle}} = \frac{1}{\sqrt{\langle z^2 \rangle}} \sqrt{\frac{\langle Z^2 \rangle}{\langle \mu \rangle}} - 1$$

FLUCTUATIONS AT SPS

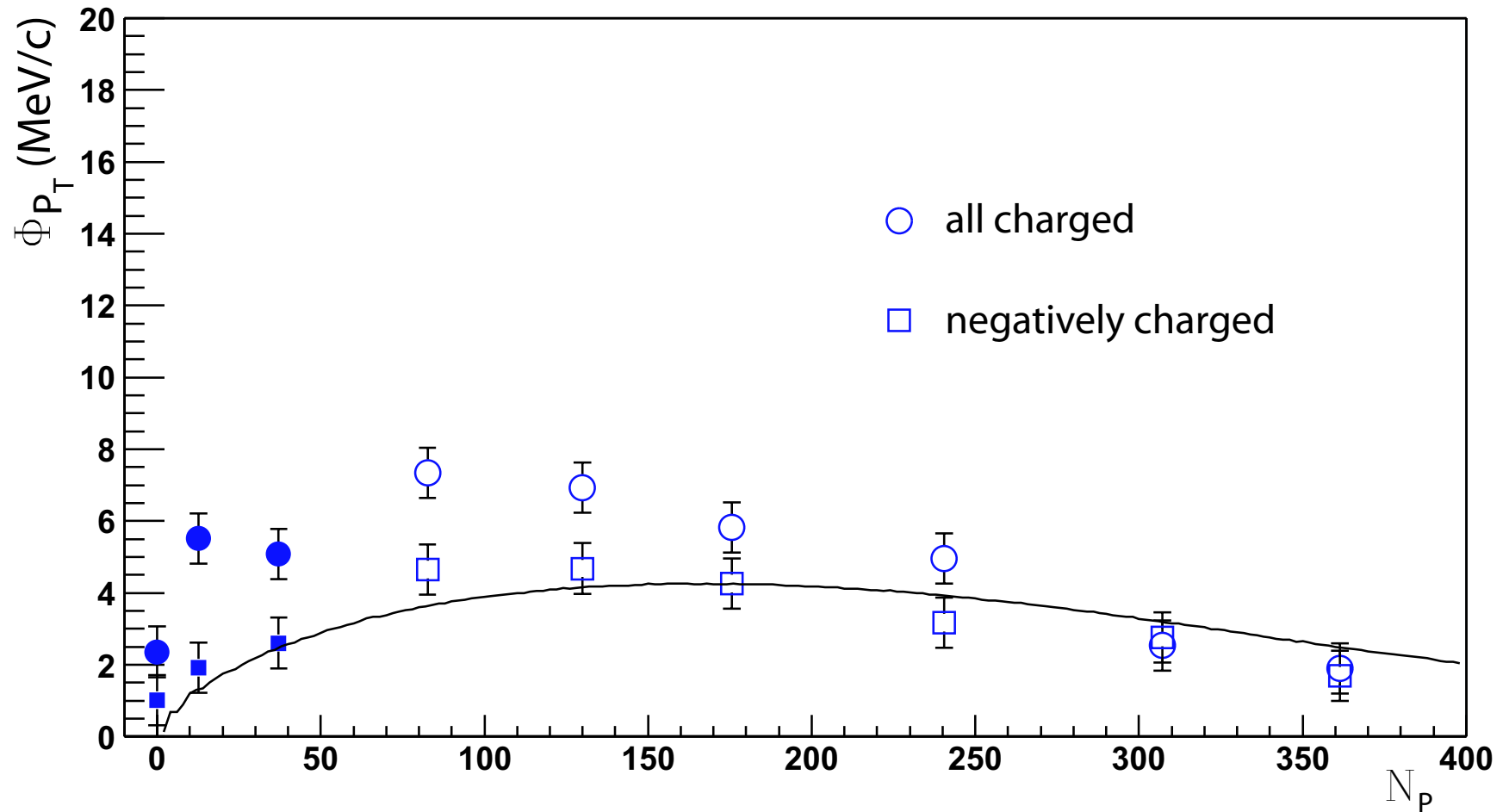


Figure 1: ϕ_{p_T} versus the number of participants. Data from NA49 Collaboration at SPS energies are compared with our results (solid line).

FLUCTUATIONS AT RHIC

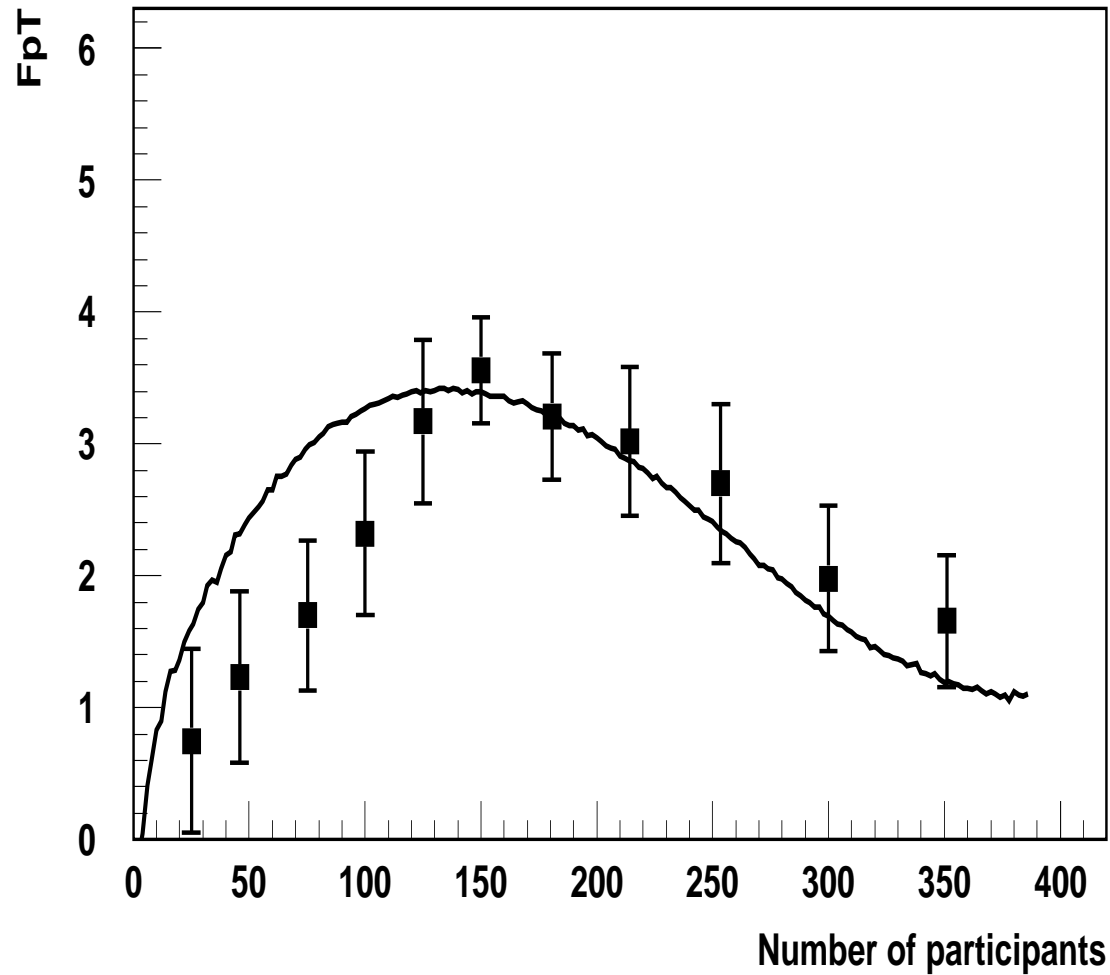


Figure 2: $F_{pT}(\%)$ versus the number of participants. Experimental data from PHENIX at $\sqrt{s} = 200$ GeV are compared with our results (solid line).

FLUCTUATIONS AT LHC

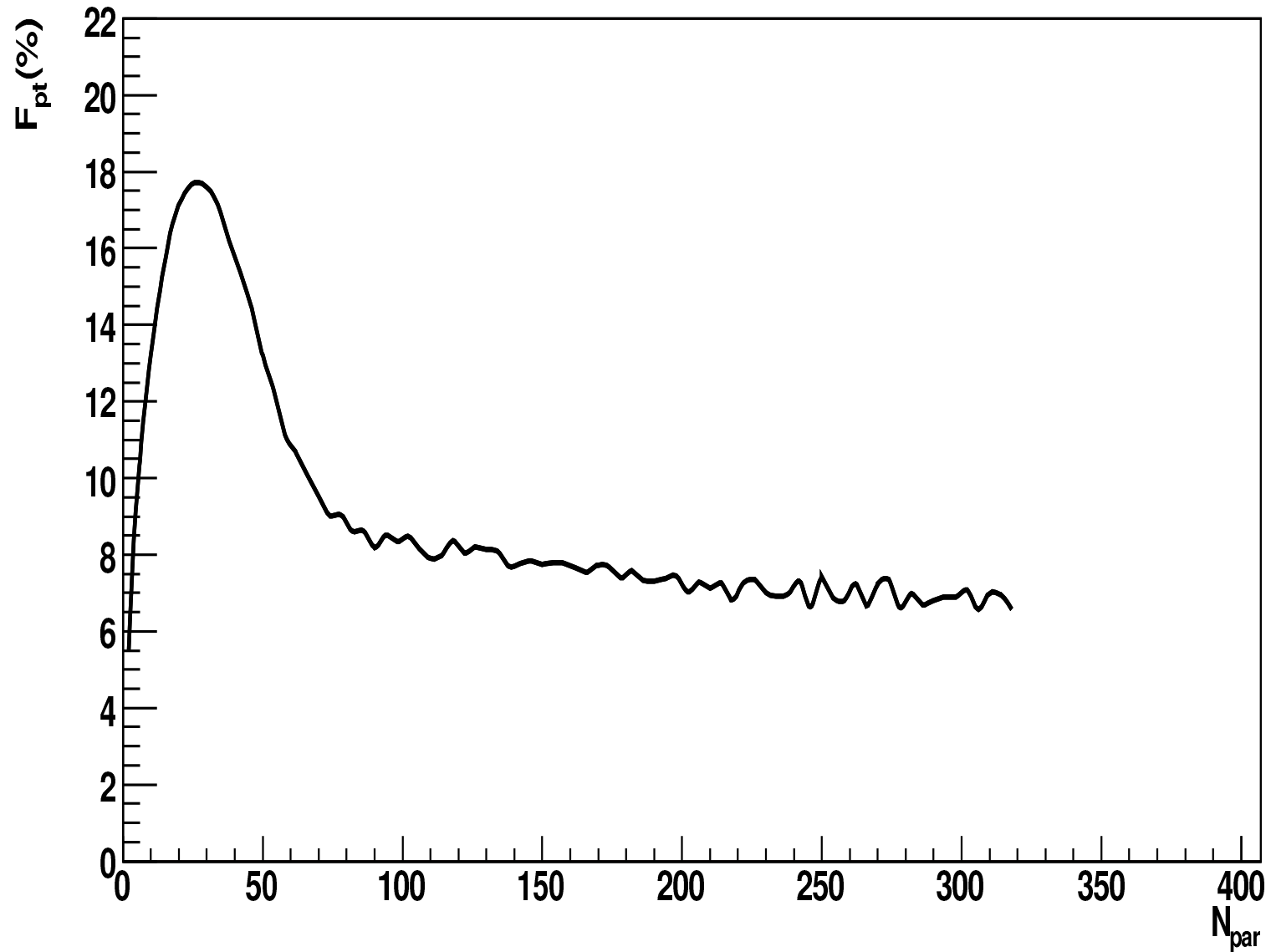


Figure 3: $F_{p_T}(\%)$ versus the number of participants at $\sqrt{s} = 5500$ GeV.

Some remarks

- The **behaviour of the transverse momentum fluctuations** with the centrality at RHIC can be explained by the **clustering of color sources**.
- In this framework, elementary color sources *–strings–* **overlap** forming clusters, so the number of effective sources is modified.
- These clusters decay into particles with mean transverse momentum that depends on the **number of elementary sources** that conform each cluster.
- The **transverse momentum fluctuations** in this approach correspond to the fluctuations of the $\langle p_T \rangle_n$ of these clusters, and behave essentially as the **number of effective sources**.
- **In a jet production scenario** the mean p_T fluctuations are attributed to jet production in peripheral events +jet suppression at larger centralities.
- **A way to discriminate between the two approaches:** fluctuations at SPS energies, where jet production cannot play a fundamental role.

EVENT-BY-EVENT MULTIPLICITY FLUCTUATIONS

- The NA49 Collaboration have presented their data on **multiplicity fluctuations as a function of centrality at SPS energies.**
- The variance of the multiplicity distribution scaled to the mean value of the multiplicity has been used.

$$Var(N) = \frac{\langle N^2 \rangle - \langle N \rangle^2}{\langle N \rangle}$$

A non-monotonic centrality –system size– dependence was found.

- **Its behaviour is similar to the one obtained for $\Phi(p_T)$**
–used by the NA49 Collaboration to quantify the p_T -fluctuations–
 \implies they are related to each other.
- The Φ -measure is independent of the distribution of number of particle sources if the sources are identical and independent from each other

FLUCTUATIONS AT SPS

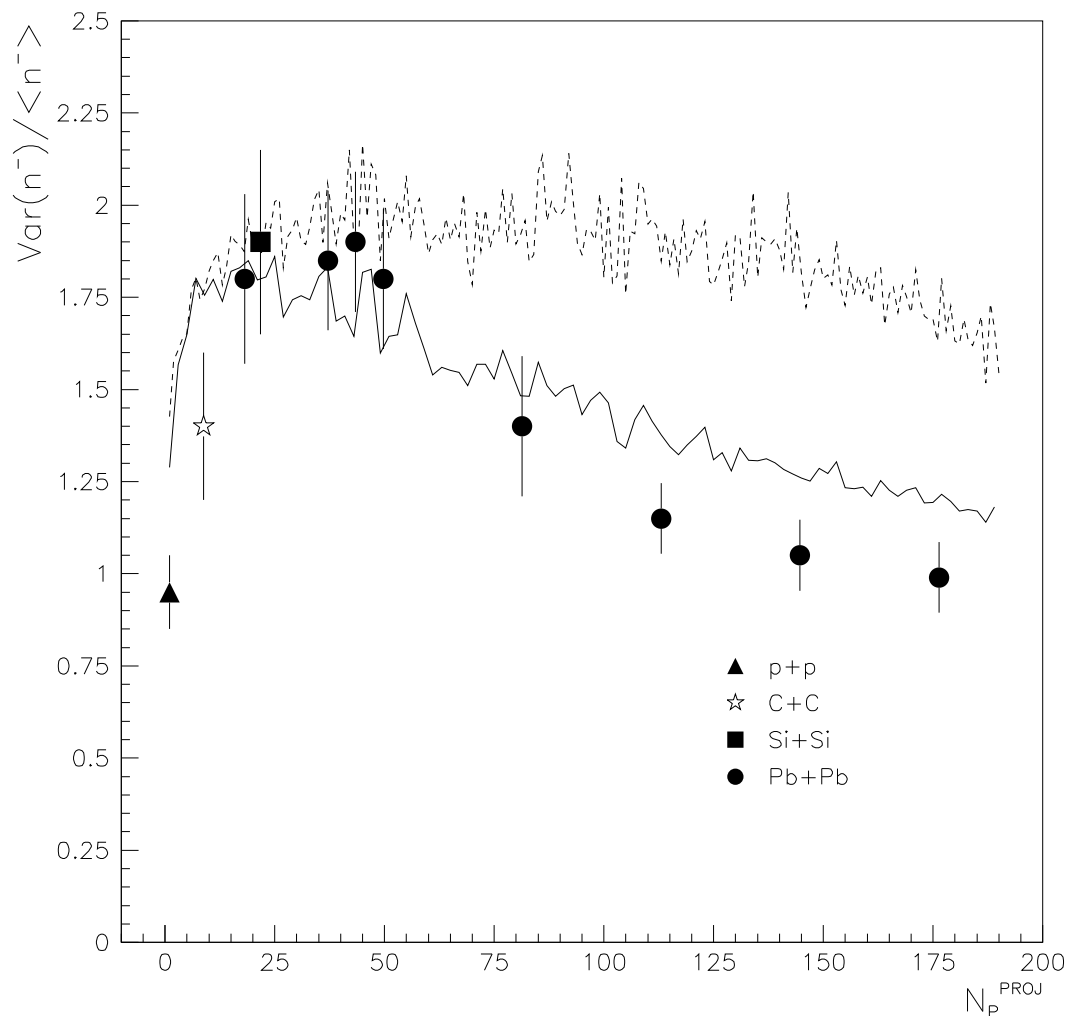


Figure 4: Scaled variance of negatively charged particles in Pb+Pb collisions at $P_{lab} = 158$ AGeV/c. The dashed line corresponds to our result without clustering, the continuous line takes into account clustering. Data: NA49.

FLUCTUATIONS AT RHIC

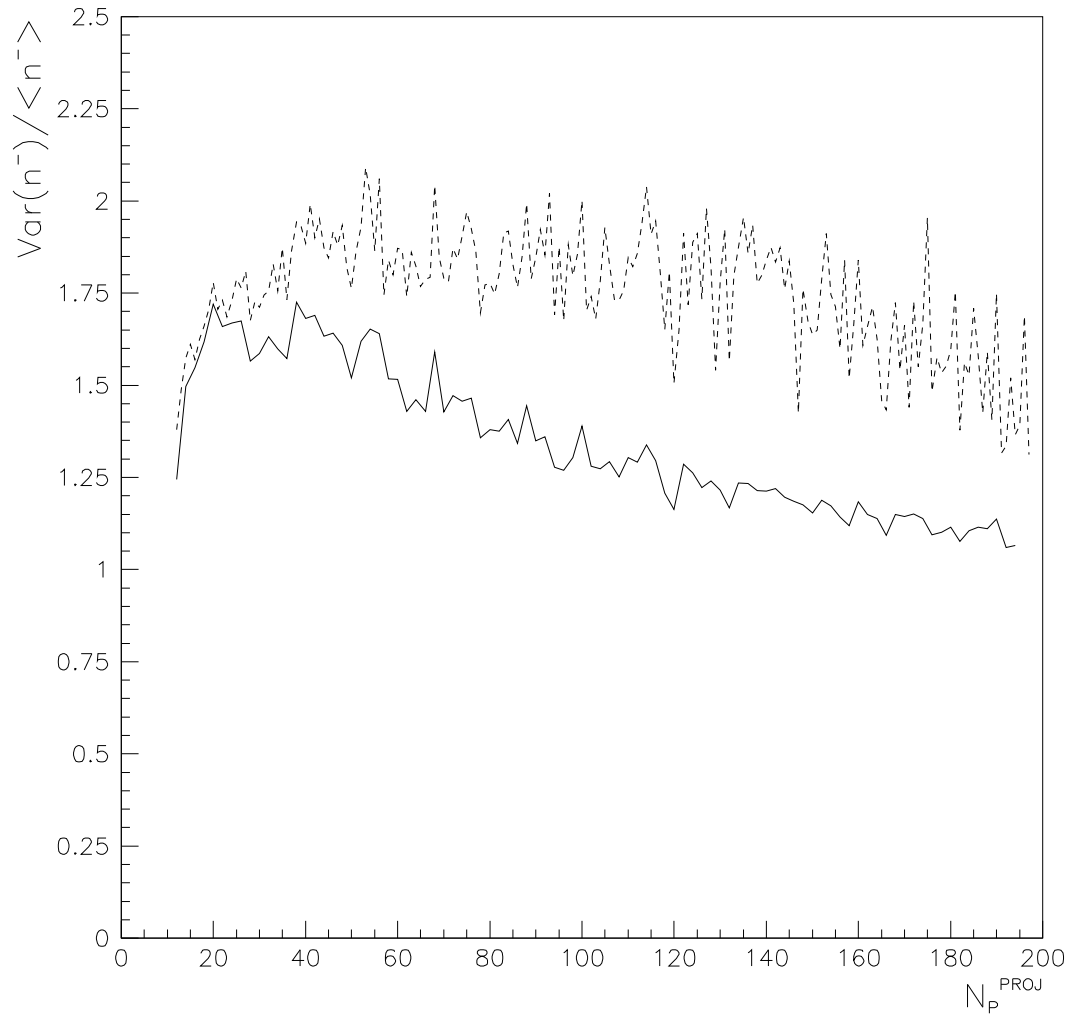


Figure 5: Scaled variance of negatively charged particles in Au+Au collisions at $\sqrt{s} = 200$ GeV. The dashed line corresponds to our result when clustering formation is not included, the continuous line takes into account clustering.

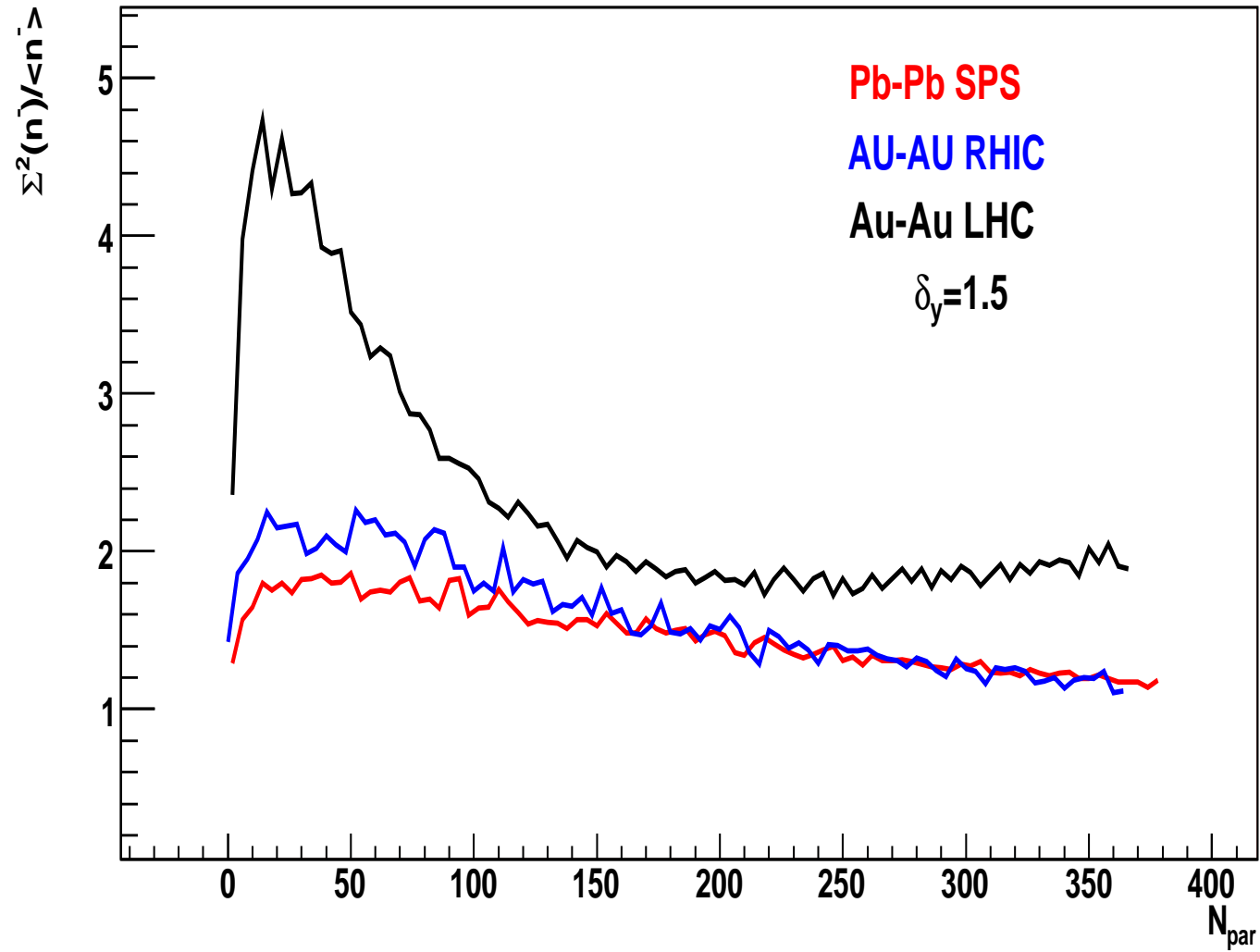


Figure 6: Our results for the scaled variance of negatively charged particles at SPS, RHIC and LHC.

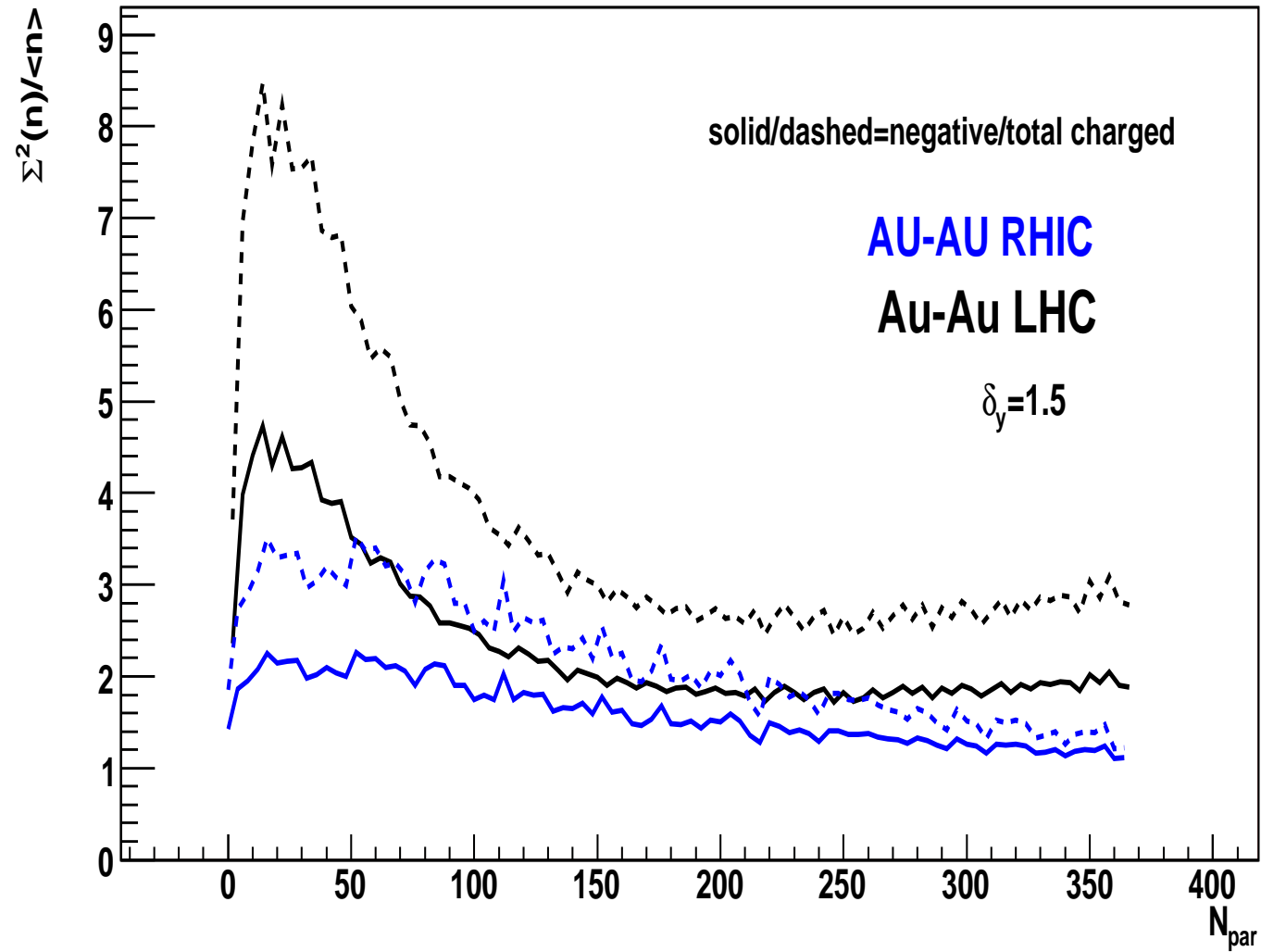


Figure 7: Our results for the scaled variance of negatively charged particles and total charged particles at SPS, RHIC and LHC energies.

- The p_T and multiplicity fluctuations are due in our approach to the different mean $\langle p_T \rangle$ and mean multiplicities of the clusters.
- The fluctuations in our approach behave essentially as the **number of clusters = number of effective sources**
 - **At low density:** most of the particles are produced by individual strings with the same $\langle p_T \rangle_1$ and the same $\langle \mu_1 \rangle$
 \Rightarrow **fluctuations are small**
 - **At large density** above the critical point: only one cluster
 \Rightarrow **fluctuations are not expected either** *"equilibration"*
 - **Just below the percolation critical density:** Large number of clusters formed by different number of strings, different size and different $\langle p_T \rangle_n$ and $\langle \mu \rangle_n$
 \Rightarrow **fluctuations are maximal**
- In other words, **a decrease in the number of effective sources leads to a decrease of the fluctuations**

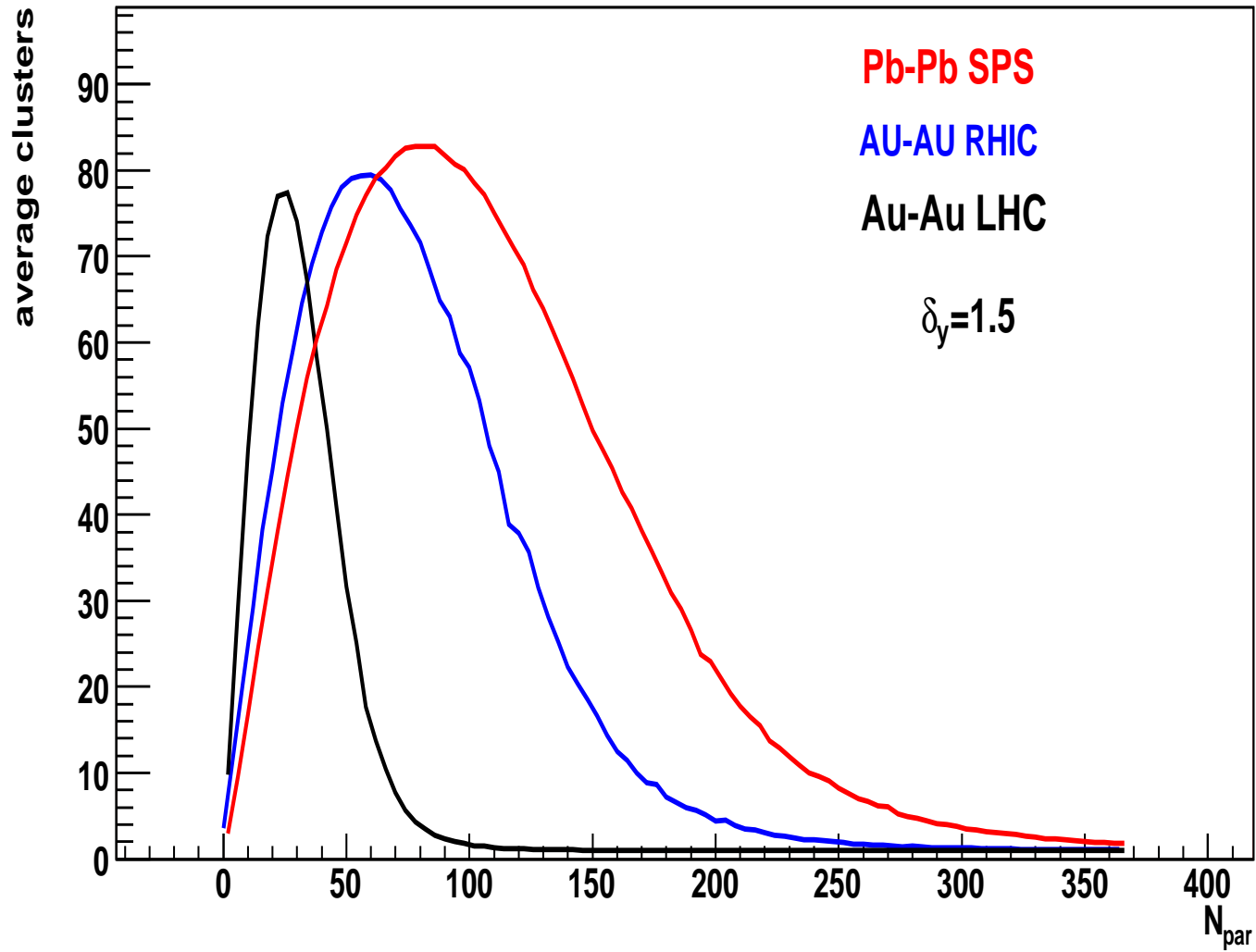


Figure 8: Average number of clusters vs centrality at SPS, RHIC and LHC.

COMMENTS

- We find a non-monotonic dependence of the multiplicity fluctuations with the number of participants.

The centrality behaviour of these fluctuations is very similar to the one found for the mean p_T fluctuations.

- In our approach, the mechanism responsible for multiplicity and mean p_T fluctuations is the formation of clusters of strings that introduces correlations between the produced particles.
- On the other hand, p_T fluctuations have been attributed to jet production in peripheral events, combined with jet suppression in central events.
- However, this hard-scattering interpretation can not be applied to SPS energies, so it does not explain the non-monotonic behaviour of the mean p_T fluctuations neither the relation between mean p_T and multiplicity fluctuations at SPS energy.
- Other possible mechanisms are: combination of strong and electromagnetic interaction, dipole-dipole interaction and non-extensive thermodynamics. Still, it is not clear if these fluctuations have a kinematic or dynamic origin, but clustering of colour sources remains a good possibility.

- Mean cluster multiplicity and mean cluster p_T :

$$\langle \mu \rangle_n = \sqrt{\frac{nS_n}{S_1}} \langle \mu \rangle_1, \quad \langle p_T \rangle_n = \left(\frac{nS_1}{S_n} \right)^{1/4} \langle p_T \rangle_1$$

where $\langle \mu \rangle_1$ and $\langle p_T \rangle_1$ correspond to the mean multiplicity and the mean transverse momentum of the particles produced by one individual string.

- In order to obtain the mean p_T and the mean multiplicity of the collision at a given centrality: sum over all clusters and average over all events:

$$\langle \mu \rangle = \frac{\sum_{i=1}^{N_{events}} \sum_j \langle \mu \rangle_{n_j}}{N_{events}}, \quad \langle p_T \rangle = \frac{\sum_{i=1}^{N_{events}} \sum_j \langle \mu \rangle_{n_j} \langle p_T \rangle_{n_j}}{\sum_{i=1}^{N_{events}} \sum_j \langle \mu \rangle_{n_j}}$$

- Introducing our formula for the multiplicity of the cluster μ_{n_j} and the mean momentum $\langle p_T \rangle_{n_j}$ we get:

$$\langle p_T \rangle = \frac{\sum_{i=1}^{N_{events}} \sum_j \left(\frac{n_j S_{n_j}}{S_1} \right)^{1/2} \mu_1 \left(\frac{n_j S_1}{S_{n_j}} \right)^{1/4} \langle p_T \rangle_1}{\sum_{i=1}^{N_{events}} \sum_j \left(\frac{n_j S_{n_j}}{S_1} \right)^{1/2} \mu_1}$$

- For the quantities $\langle z^2 \rangle$ and $\langle Z^2 \rangle$ we obtain:

$$\langle z^2 \rangle = \frac{\sum_{i=1}^{N_{events}} \sum_j \left(\frac{n_j S_{n_j}}{S_1} \right)^{1/2} \mu_1 \left[\left(\frac{n_j S_1}{S_{n_j}} \right)^{1/4} \langle p_T \rangle_1 - \langle p_T \rangle \right]^2}{\sum_{i=1}^{N_{events}} \sum_j \left(\frac{n_j S_{n_j}}{S_1} \right)^{1/2} \mu_1}$$

and

$$\frac{\langle Z^2 \rangle}{\langle \mu \rangle} = \frac{\sum_{i=1}^{N_{events}} \left[\sum_j \left(\frac{n_j S_{n_j}}{S_1} \right)^{1/2} \mu_1 \left[\left(\frac{n_j S_1}{S_{n_j}} \right)^{1/4} \langle p_T \rangle_1 - \langle p_T \rangle \right] \right]^2}{\sum_{i=1}^{N_{events}} \sum_j \left(\frac{n_j S_{n_j}}{S_1} \right)^{1/2} \mu_1}$$

$$F_{p_T} = \frac{\phi}{\sqrt{\langle z^2 \rangle}} = \frac{1}{\sqrt{\langle z^2 \rangle}} \sqrt{\frac{\langle Z^2 \rangle}{\langle \mu \rangle}} - 1$$

In order to compute F_{p_T} we need:

- A **Monte Carlo code for the cluster formation**, in order to compute the number of strings that come into each cluster and the area of the cluster
- We do not use a Monte Carlo code for the decay of the cluster, since we apply **analytical expressions for the transverse momentum and the multiplicities** of the clusters
- We also need **the value of μ_1** –multiplicity produced by one individual string–. The total multiplicity per unit rapidity produced by one string has been taken as $\mu_{0\,tot} \simeq 1$

- In order to compute our value for F_{p_T} , we take into account all possible transverse momenta, whereas in the experiment there is a limited acceptance, $0.2 \text{ GeV}/c < p_T < p_T^{max}$
- PHENIX has studied the variation of F_{p_T} with the maximal value of the acceptance for p_T , p_T^{max} . The maximum of F_{p_T} is reached for the largest acceptance, $p_T^{max} = 4 \text{ GeV}/c$
- So we can expect that our value for F_{p_T} is going to be higher than the experimental one, specially for a moderate number of participants, N_p , since the truncated average $p_T, < p_T^{trunc} > = \frac{\int_{p_T^{min}}^{\infty} p_T dN/dp_T}{\int_{p_T^{min}}^{\infty} dN/dp_T} - p_T^{min}$, decreases with the number of participants for $p_T^{min} > 2 \text{ GeV}/c$
- This means that, for momenta higher than $2 \text{ GeV}/c$, the high p_T contribution would be due to collisions with a moderate number of participants
- These considerations may explain the difference between our results and PHENIX data with a limited acceptance of $0.2 < p_T < 2 \text{ GeV}$ at low N_p

- In order to have a better understanding of the behaviour of F_{p_T} and ϕ_{p_T} on the number of participants, we plot in Fig. 9 and Fig. 10 the mean number of clusters M and the dispersion on the number of clusters multiplied by the number of clusters $\sigma_M * M$ at RHIC and SPS energies.
- The p_T fluctuations are due in our approach to the different mean transverse momenta of the clusters. These momenta depend on the number of strings that comes into the cluster and the area occupied by the cluster, therefore M and σ_M should be the key quantities.
- The only effect of σ_M is to shift the maximum of M . Because of this we expect the dependence of F_{p_T} and ϕ_{p_T} on N_p to be more similar to the M behaviour, as it is actually.
- In other words, a decrease in the number of effective sources leads to a decrease of the transverse momentum fluctuations.

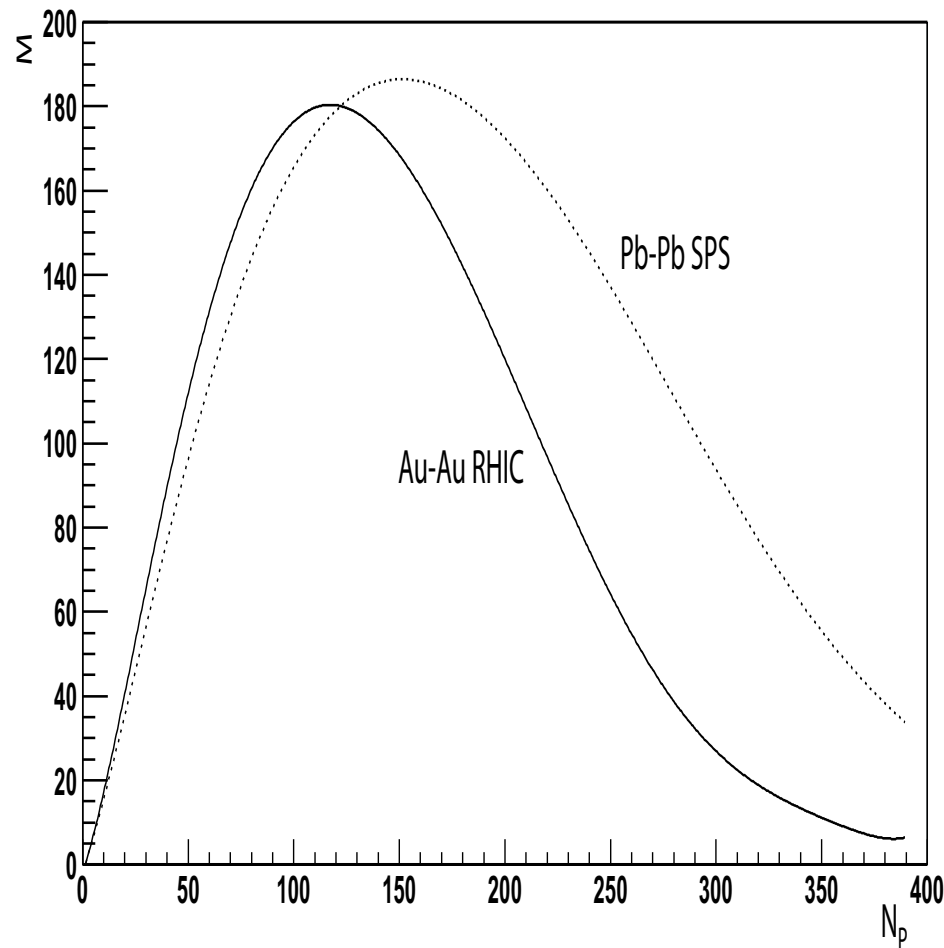


Figure 9: Mean number of clusters M versus the number of participants for Pb-Pb collisions at SPS energies (dotted line) and Au-Au collisions at RHIC energies (solid line).

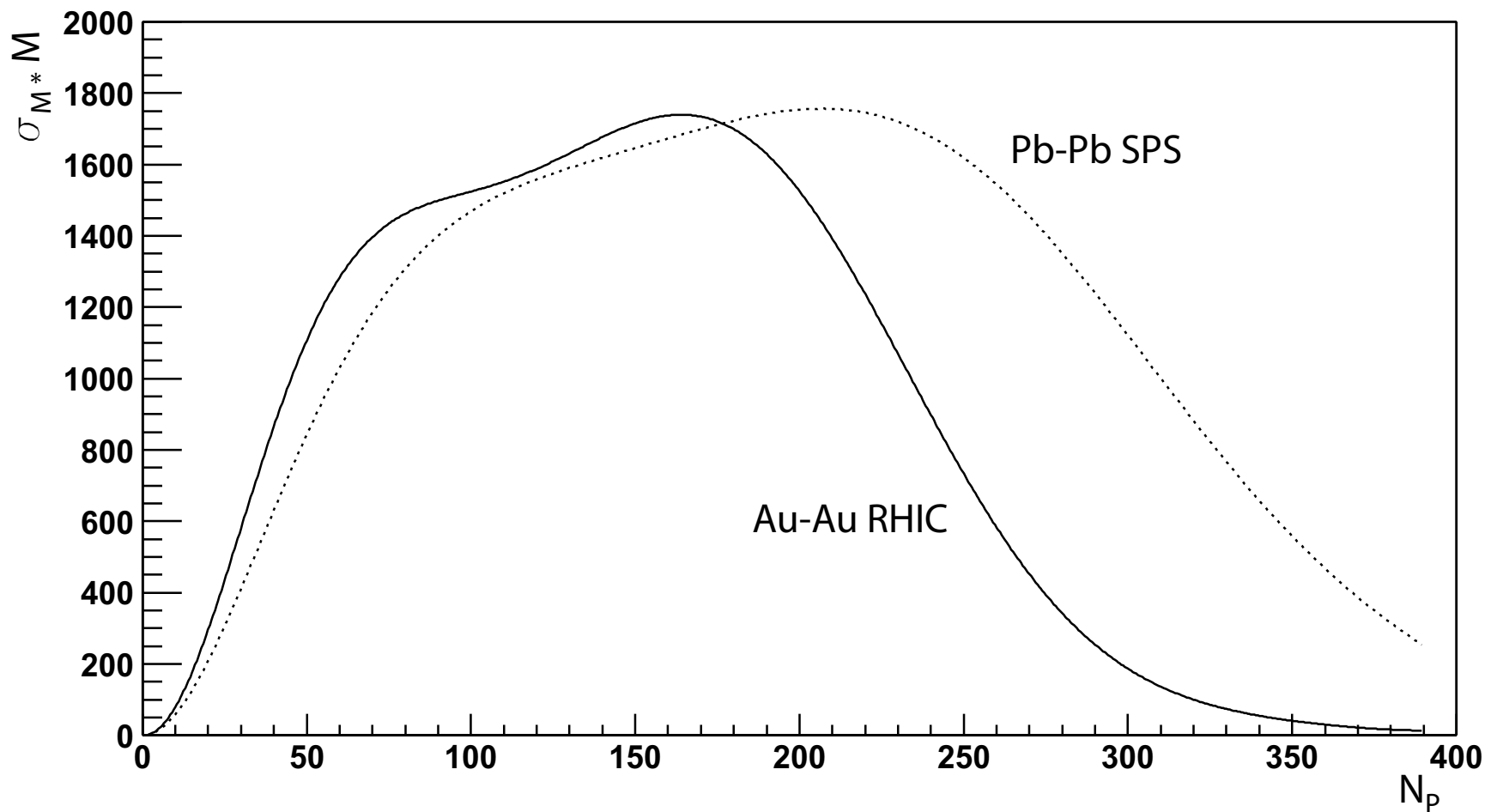


Figure 10: Dispersion on the number of clusters multiplied by the number of clusters $\sigma_M * M$ versus the number of participants for Pb-Pb collisions at SPS energies (dotted line) and Au-Au collisions at RHIC energies (solid line).

Our formula for the scaled variance obeys:

$$\frac{Var(\mu)}{\langle \mu \rangle} = 1 + \langle \mu \rangle_1 \frac{\left\langle \left(\sum_j \sqrt{\frac{n_j S_{n_j}}{S_1}} \right)^2 \right\rangle - \left\langle \sum_j \sqrt{\frac{n_j S_{n_j}}{S_1}} \right\rangle^2}{\left\langle \sum_j \sqrt{\frac{n_j S_{n_j}}{S_1}} \right\rangle},$$

In order to obtain the scaled variance we have calculated $\langle \mu^2 \rangle$:

$$\langle \mu^2 \rangle = \frac{1}{N_{events}} \left[\sum_{i=1}^{N_{events}} \left(\sum_j \sqrt{\frac{n_j S_{n_j}}{S_1}} \right)^2 \langle \mu \rangle_1^2 + \sum_{i=1}^{N_{events}} \sum_j \sqrt{\frac{n_j S_{n_j}}{S_1}} \langle \mu \rangle_1 \right]$$

where we have supposed that the multiplicity of each cluster follows a Poissonian of mean value $\langle \mu \rangle_{n_j}$, $\langle \mu^2 \rangle_{n_j} = \langle \mu \rangle_{n_j}^2 + \langle \mu \rangle_{n_j}$.

Behaviour of the scaled varianza

- **Low density limit** –isolated strings that do not interact–:

$$\frac{Var(\mu)}{\langle \mu \rangle} = 1 + \langle \mu \rangle_1 \frac{\langle N_s^2 \rangle - \langle N_s \rangle^2}{\langle N_s \rangle} \simeq 1 + \langle \mu \rangle_1$$

where N_s corresponds to the number of strings that, for a fixed number of participants:
 $\frac{\langle N_s^2 \rangle - \langle N_s \rangle^2}{\langle N_s \rangle} \simeq 1$ (Poissonian distribution).

- **In the large density regime** –all the strings fuse into a single cluster that occupies the whole interaction area–:

$$\frac{Var(\mu)}{\langle \mu \rangle} = 1 + \langle \mu \rangle_1 \frac{\left\langle \left(\sqrt{\frac{N_s S_A}{S_1}} \right)^2 \right\rangle - \left\langle \sqrt{\frac{N_s S_A}{S_1}} \right\rangle^2}{\left\langle \sqrt{\frac{N_s S_A}{S_1}} \right\rangle} \simeq 1$$

where S_A is the nuclear overlap area.

The second element of the r.h.s. of this equation tends to zero.

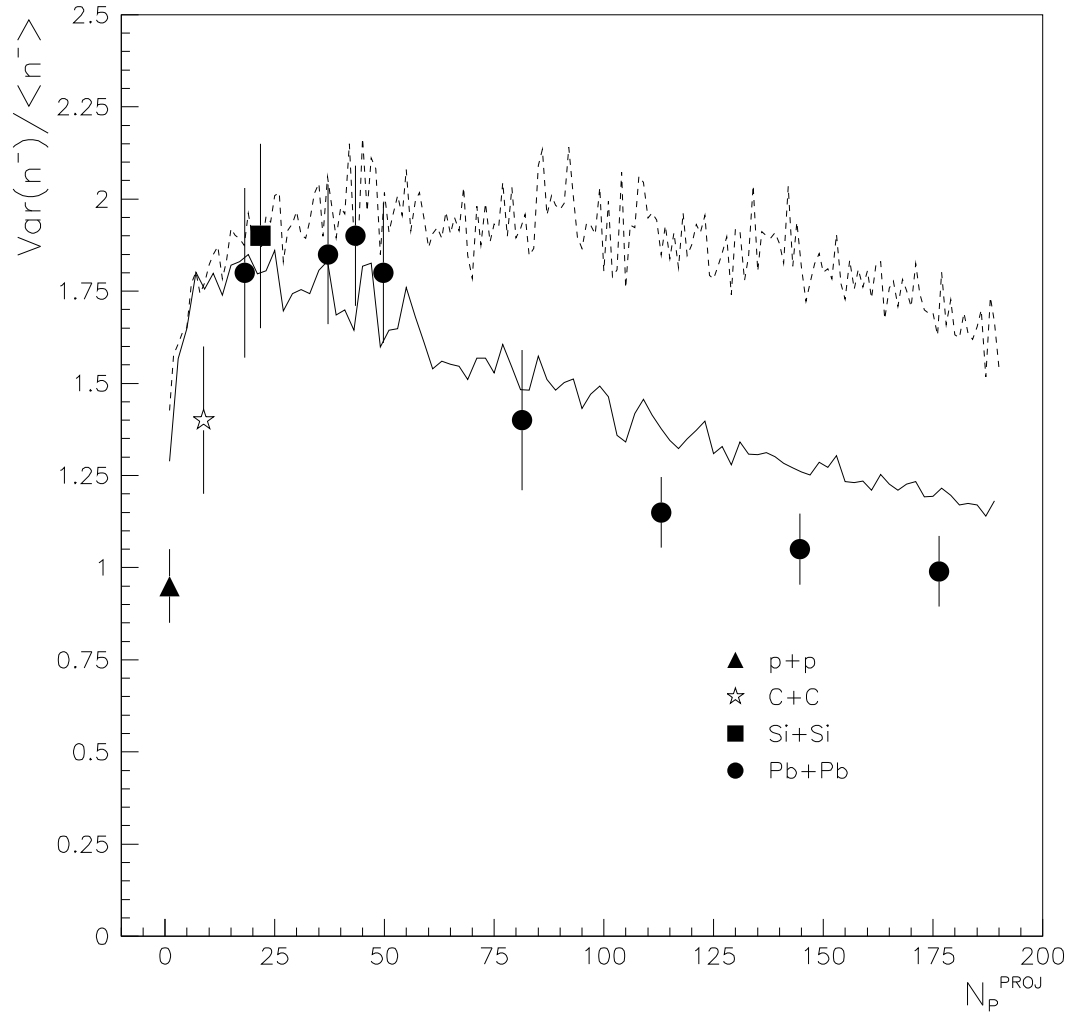


Figure 11: Our results for the scaled variance of negatively charged particles in Pb+Pb collisions at $P_{lab} = 158$ AGeV/c compared to NA49 experimental data. The dashed line corresponds to our result when clustering formation is not included, the continuous line takes into account clustering.

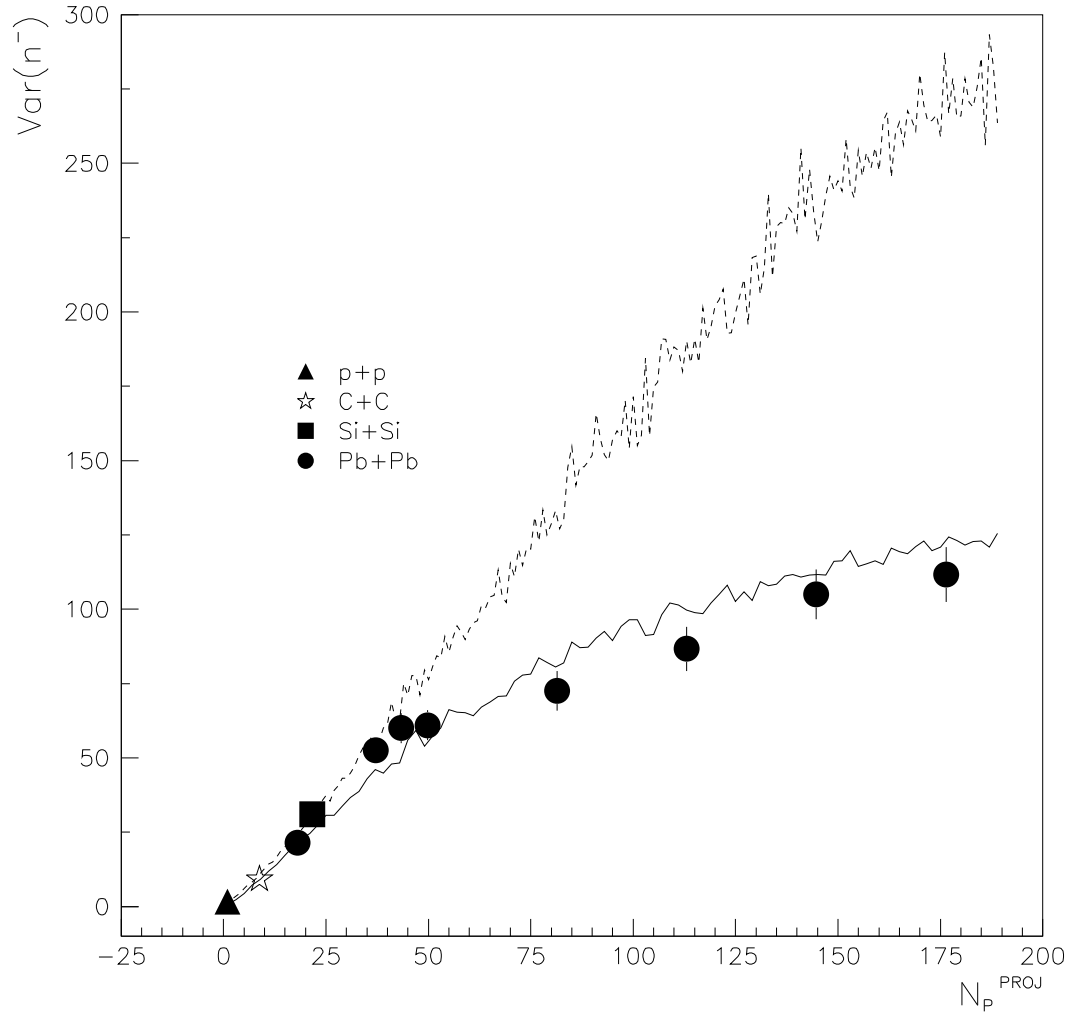


Figure 12: Our results for the variance of negatively charged particles in Pb+Pb collisions at $P_{lab} = 158$ AGeV/c compared to NA49 experimental data. The dashed line corresponds to our result when clustering formation is not included, the continuous line takes into account clustering.

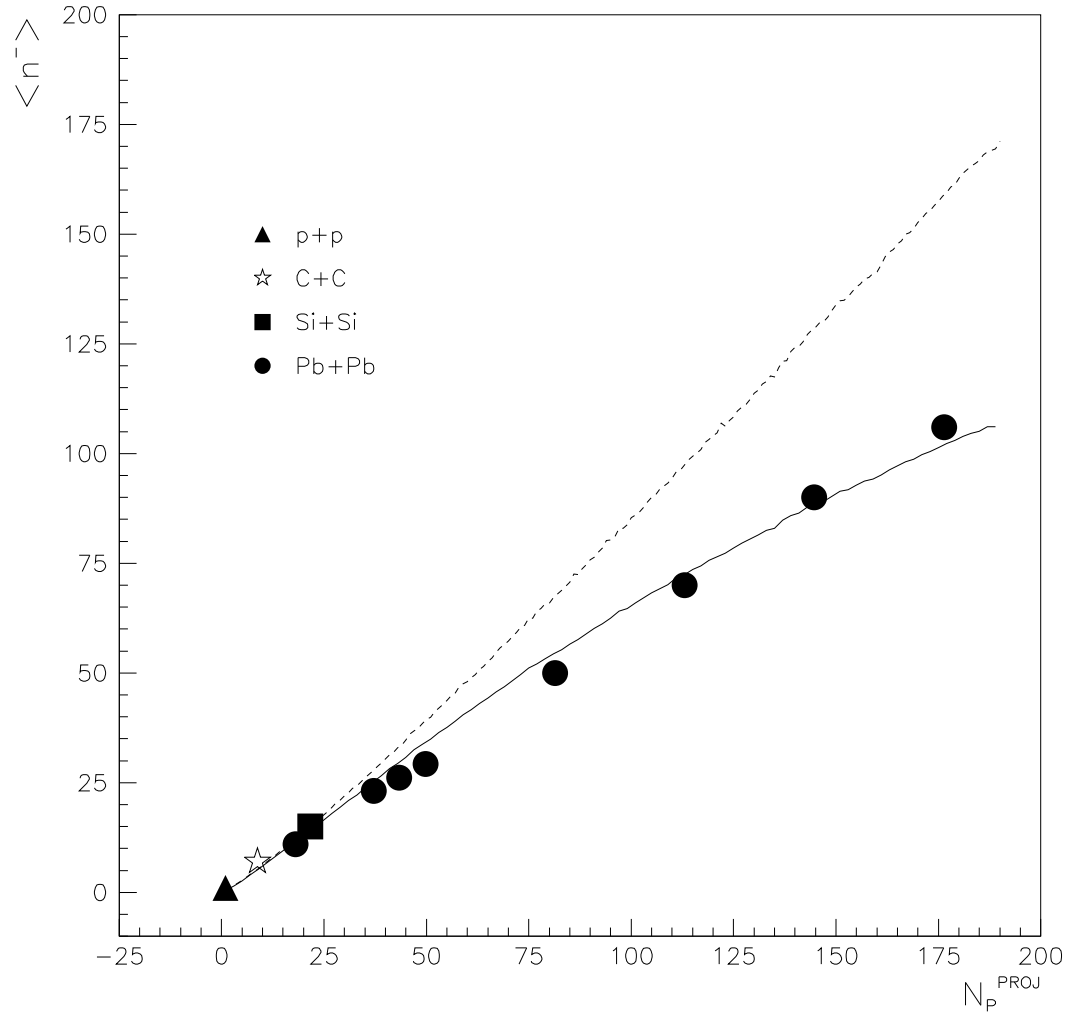


Figure 13: Our results for the mean multiplicity of negatively charged particles in Pb+Pb collisions at $P_{lab} = 158$ AGeV/c compared to NA49 experimental data. The dashed line corresponds to our result when clustering formation is not included, the continuous line takes into account clustering₃₂

LONG AND SHORT RANGE CORRELATIONS

- A measurement of such correlations is the backward–forward dispersion

$$D_{BF}^2 = \langle n_B n_F \rangle - \langle n_B \rangle \langle n_F \rangle$$

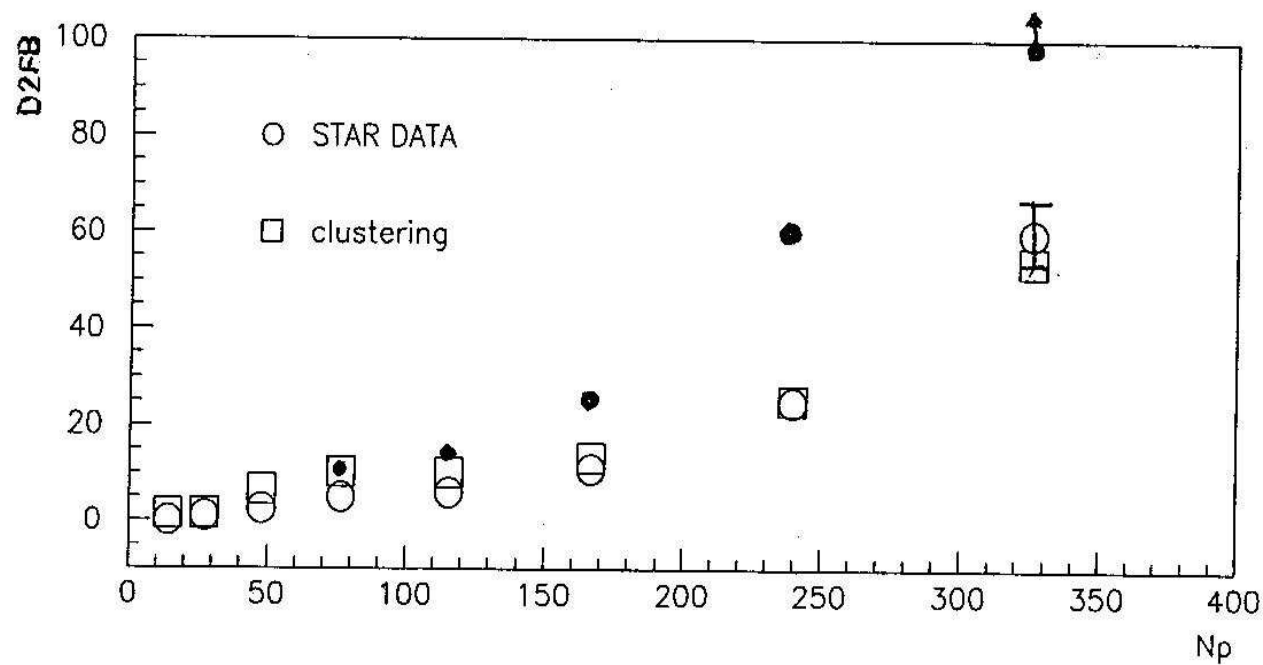
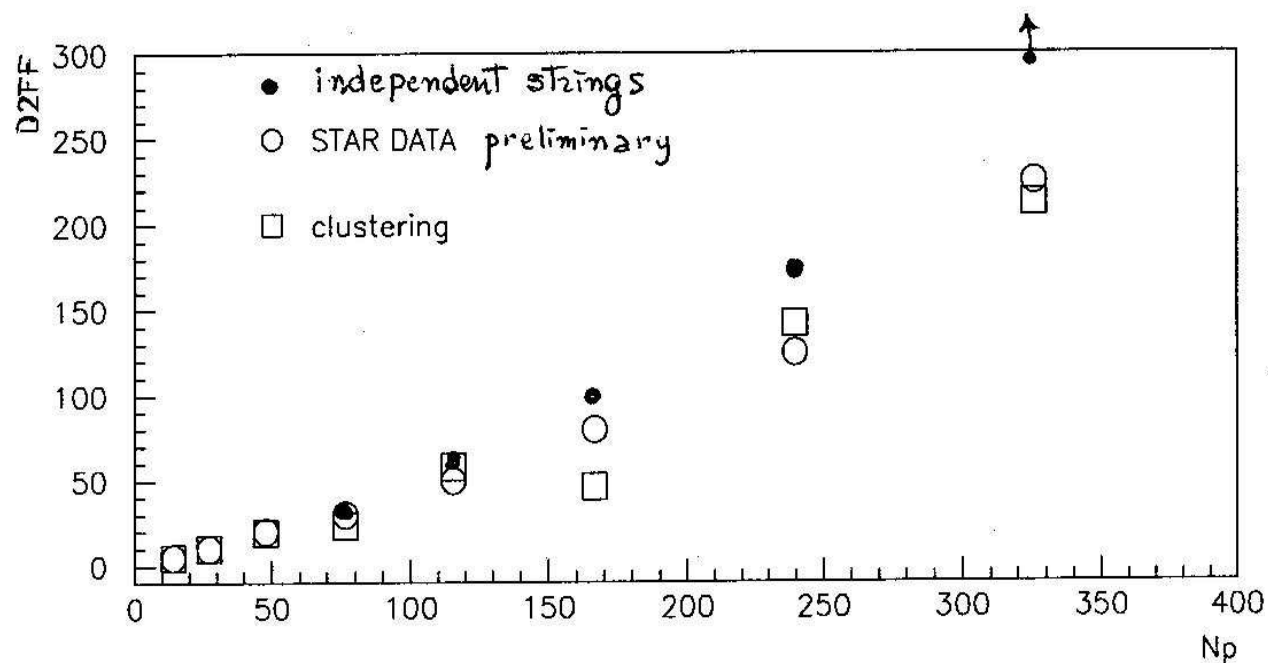
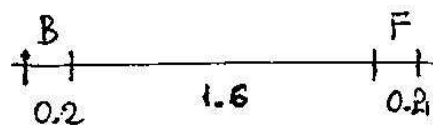
where n_B (n_F) is the number of particles in a backward (forward) rapidity

- In a superposition of independent sources model, D_{BF}^2 is proportional to the fluctuations on the number of independent sources
- Cluster formation implies a decreasing number of independent sources:
 \implies Reduction of long range correlations with increasing collectivity
- A measure of the clustering:

$$b = D_{BF}^2 / D_{FF}^2$$

Similar results in the framework of the CGC

Armesto, McLerran and Pajares, hep-ph/0607345



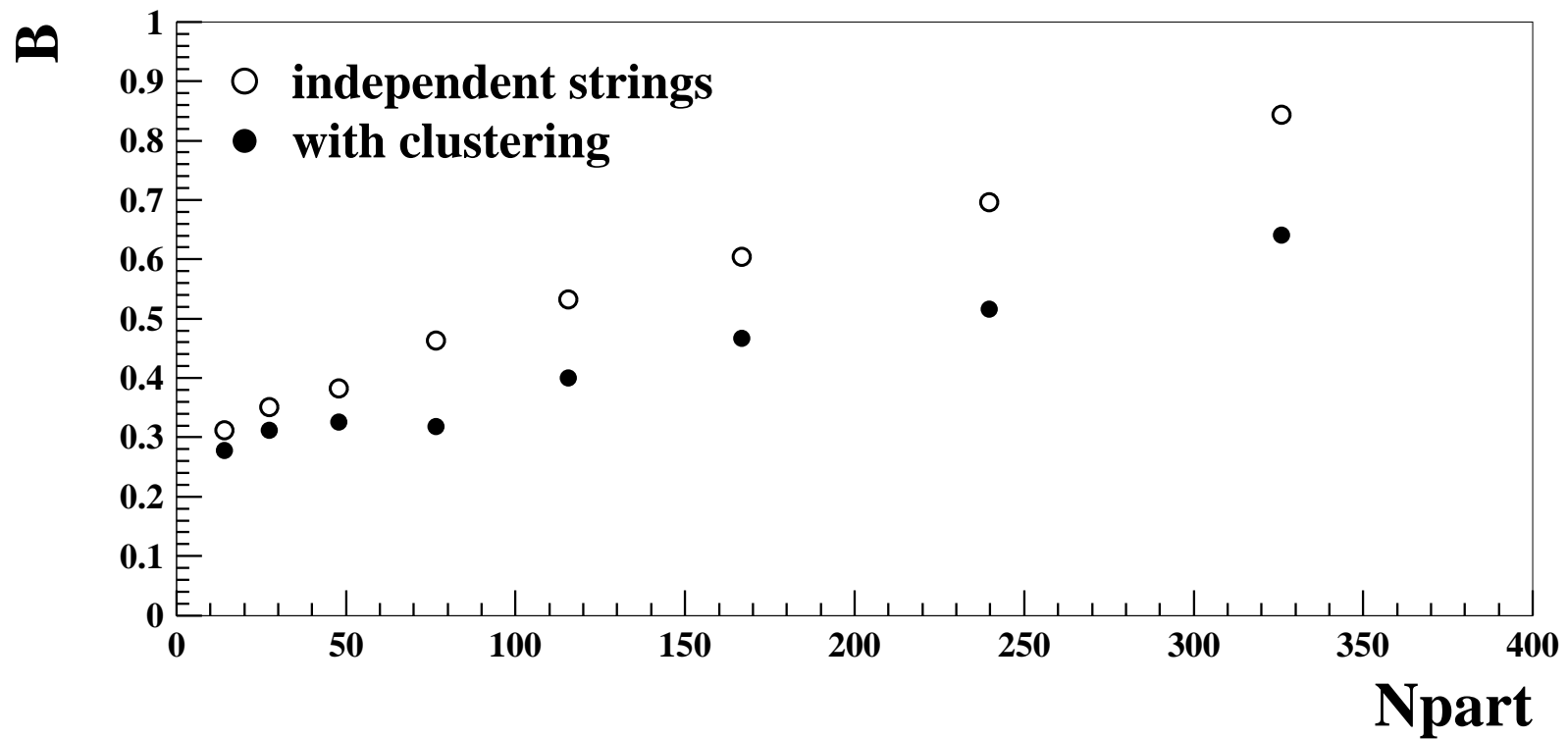


Figure 14: **LONG AND SHORT RANGE CORRELATIONS AT RHIC**

